A&A 604, A26 (2017)
DOI: 10.1051/0004-6361/201629725

Astronomy & Astrophysics

Doubly ^{15}N-substituted diazenylium: THz laboratory spectra and fractionation models

L. Dore[1], L. Bizzocchi[2], E. S. Wirström[4], C. Degli Esposti[1], F. Tamassia[3], and S. B. Charnley[5]

[1] Dipartimento di Chimica "Giacomo Ciamician", Università di Bologna, via F. Selmi 2, 40126 Bologna, Italy
e-mail: luca.dore@unibo.it
[2] Centre for Astrochemical Studies, Max-Planck-Institut für extraterrestrische Physik, Gießenbachstraße 1, 85749 Garching bei München, Germany
e-mail: bizzocchi@mpe.mpg.de
[3] Dipartimento di Chimica Industriale "Toso Montanari", Università di Bologna, Viale del Risorgimento 4, 40136 Bologna, Italy
[4] Department of Earth and Space Sciences, Chalmers University of Technology, Onsala Space Observatory, 439 92 Onsala, Sweden
e-mail: eva.wirstrom@chalmers.se
[5] Astrochemistry Laboratory and The Goddard Center for Astrobiology, NASA Goddard Space Flight Center, Greenbelt, MD 20770, USA

Received 16 September 2016 / Accepted 28 April 2017

ABSTRACT

Context. Isotopic fractionation in dense molecular cores has been suggested as a possible origin of large $^{14}N/^{15}N$ ratio variations in solar system materials. While chemical models can explain some observed variations with different fractionation patterns for molecules with –NH or –CN functional groups, they fail to reproduce the observed ratios in diazenylium (N_2H^+).
Aims. Observations of doubly ^{15}N-substituted species could provide important constraints and insights for theoretical chemical models of isotopic fractionation. However, spectroscopic data are very scarce.
Methods. The rotational spectra of the fully ^{15}N-substituted isopologues of the diazenylium ion, $^{15}N_2H^+$ and $^{15}N_2D^+$, have been investigated in the laboratory well into the THz region by using a source-modulation microwave spectrometer equipped with a negative glow discharge cell. An extended chemical reaction network has been used to estimate what ranges of ^{15}N fractionation in doubly ^{15}N-substituted species could be expected in the interstellar medium (ISM).
Results. For each isotopologue of the H- and D-containing pair, nine rotational transitions were accurately measured in the frequency region 88 GHz–1.2 THz. The analysis of the spectrum provided very precise rest frequencies at millimeter and sub-millimeter wavelengths, useful for the radioastronomical identification of the rotational lines of $^{15}N_2H^+$ and $^{15}N_2D^+$ in the ISM.

Key words. astrochemistry – molecular data – methods: laboratory: molecular – techniques: spectroscopic – ISM: molecules

1. Introduction

The $^{14}N/^{15}N$ isotopic ratio for atmospheric N_2 is 273 ± 1 (Nier 1950), a value comparable to that of the local interstellar medium (ISM) obtained from observations in objects where nitrogen fractionation should be negligible: 274 ± 18 estimated from the $C^{14}N/C^{15}N$ ratio in diffuse molecular clouds (Ritchey et al. 2015), and 290 ± 40 derived from the gradient of the $^{14}N/^{15}N$ ratio in the Galaxy observed towards warm molecular clouds (Adande & Ziurys 2012).

However, in the solar system the nitrogen isotope composition varies over a broad range of values of $^{14}N/^{15}N$: from 441 ± 6, the elemental ratio of the protosolar nebula (Marty et al. 2011), to 46 ± 2 in hotspots of the *Isheyevo* meteorite (Briani et al. 2009). The $^{14}N/^{15}N$ ratios measured in comets also show high enrichments in ^{15}N (Mumma & Charnley 2011; Bockelée-Morvan et al. 2015). While the processes of nitrogen fractionation responsible for this variation are still under debate (Füri & Marty 2015), one possibility is disequilibrium ion-molecule reactions in cold, dense regions of the presolar nebula (e.g., Terzieva & Herbst 2000; Rodgers & Charnley 2008).

In dark molecular cloud cores the $^{14}N/^{15}N$ values span a wide range, where in general nitriles (HCN, HNC) show ^{15}N enrichments, ammonia mostly shows depletion, and diazenylium ions (N_2H^+) show the highest depletion (see summary in Wirström et al. 2015) with, for example, $^{14}N/^{15}N$ = 1000 ± 200 in the starless cloud core L1544 (Bizzocchi et al. 2013). Recent observations toward 26 massive star-forming cores in different evolutionary stages show for the first time ^{15}N enhancements in diazenylium, with values ranging from ~180 up to ~1300 (Fontani et al. 2015). The same objects typically show different $^{14}N/^{15}N$ ratios depending on the molecule observed, and spatial variations within cores are also observed, as for L1544 where the $^{14}N/^{15}N$ ratio in HCN varies in the range 140–360 (Hily-Blant et al. 2013). The discrepancy between ratios in the same cold core is explained in chemical models by the different gas-phase formation paths, and therefore different origins of the ^{15}N fractionation, of molecules with –NH or –CN functional groups (Wirström et al. 2012). These models, however, predict a ^{15}N enhancement in diazenylium at all evolutionary stages. In a more recent study, Roueff et al. (2015) found that the "main" N fractionation reaction, $^{15}N + N_2H^+$, does have an entrance barrier, and their chemical model therefore predicts the $^{14}N/^{15}N$ ratio in N_2H^+ to remain close to the elemental value.

The wide ranges of observed $^{14}N/^{15}N$ ratios in interstellar N_2H^+ currently present a major challenge for models of N fractionation. The chemical reaction networks of both

Wirström et al. (2012) and Roueff et al. (2015) include $^{15}N_2$ and other species containing two ^{15}N atoms in their networks, but do not consider fractionation in the reactions forming these molecules, which could potentially result in substantial shifts in the $^{15}N_2H^+/^{15}NNH^+/N^{15}NH^+/N_2H^+$ abundance relations. Detections of doubly ^{15}N-substituted species would provide a crucial constraint for these models, but spectroscopic data are almost completely lacking.

In practical terms, the diazenylium ion is the only feasible astrochemical tracer bearing two N atoms. A large body of rotational data is available for its normal species, N_2H^+ (Yu et al. 2009, and references therein), and ground-state rotational spectra of the singly ^{15}N-substituted isotopologues ($^{15}NNH^+$ and $N^{15}NH^+$) are also well characterized (Dore et al. 2009; Yu et al. 2009). Moreover, deuterated isotopologues have been detected by millimeter-wave spectroscopy (see Yu et al. 2009, and references therein). For the $^{15}N_2H^+$ isotopologue, on the other hand, only the $J = 1 \leftarrow 0$ transition has been reported (Gudeman 1982), while $^{15}N_2D^+$ has never been detected in the laboratory. The present paper fills the gap, reporting the ground-state rotational spectra of these two doubly ^{15}N substituted isotopologues up to the Terahertz region.

2. Experimental details and data analysis

The frequency-modulated (FM) absorption spectrometer used in this work is equipped with a negative glow discharge cell made of a Pyrex tube (3.25 m long and 5 cm in diameter) in order to synthesize in situ the substituted diazenylium ion. The radiation source can cover the millimeter- and submillimeter-wave region by frequency multiplication (×3, ×4, ×6, ×8, or ×9) of a series of Gunn oscillators working in the regions 75–105 GHz and 114–133 GHz. The frequency stabilization of the Gunn oscillator is achieved by locking it to a centimeter-wave synthesizer, driven by a 5 MHz-rubidium frequency standard, by means of one phase-lock loop. FM is obtained by sine-wave modulating at 6 kHz the reference signal of the wide-band Gunn-synchronizer. Lock-in detection at $2f$ of the signal from a liquid-helium-cooled InSb hot electron bolometer provides a "second derivative" profile of the observed transition lines.

The molecular ion $^{15}N_2H^+$, or $^{15}N_2D^+$, was produced by a direct-current discharge of a few mA across two cylindrical hollow steel electrodes placed at either end of the cell, while a 1:1 mixture of $^{15}N_2$ and H_2, or D_2, was flowing in Ar buffer gas. Cooling of the cell walls at ~80 K, by liquid nitrogen circulation, and magnetic confinement, by a 110 G axial field throughout the length of the discharge, provided the best conditions for the production of the diazenylium ion. No Doppler shift, due to the drift velocity of the absorbing species, should affect the transition frequencies, since the region of the low-density plasma where ions form, the negative glow, is a nearly field-free region. In addition, the nitrogen hyperfine structure is absent, since the ^{15}N isotope has spin $\frac{1}{2}$, therefore recovering the transition frequency from the spectrum is straightforward by a line shape analysis of the experimental profile modeled as a Voigt function (see Fig. 1). However, pressure shift can perturb the line center: it is indeed a tiny effect, except for the $J = 1 \leftarrow 0$ transition (Cazzoli et al. 2012). The test shown in Fig. 2 confirms that its center frequency can shift by 20–30 kHz when the measurement is carried out at the usual buffer-gas pressure of about 10 mTorr, as was the case of Gudeman (1982), who determined a transition frequency of 88 264.083 MHz, which differs by +25 kHz from the present determination of $^{15}N_2H^+$ (1–0) at the limit of zero Ar pressure.

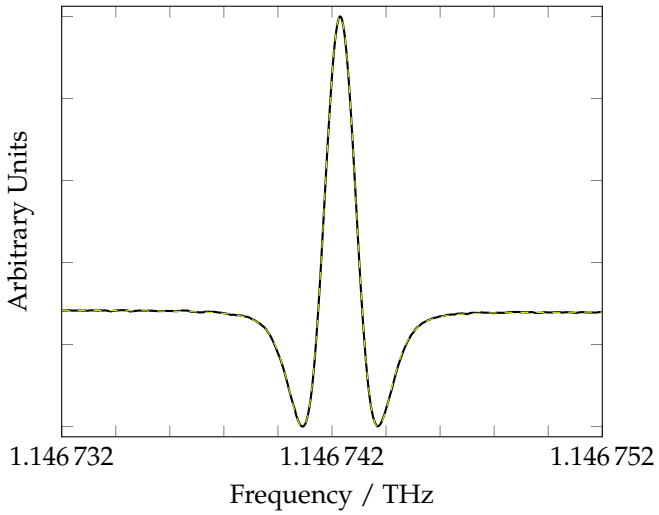

Fig. 1. Spectrum of the $J = 13 \leftarrow 12$ transition of $^{15}N_2H^+$ (solid black line) and fitted profile (dashed lime line); total integration time: 300 s; scanning rate: 0.66 MHz/s; modulation depth: 900 kHz.

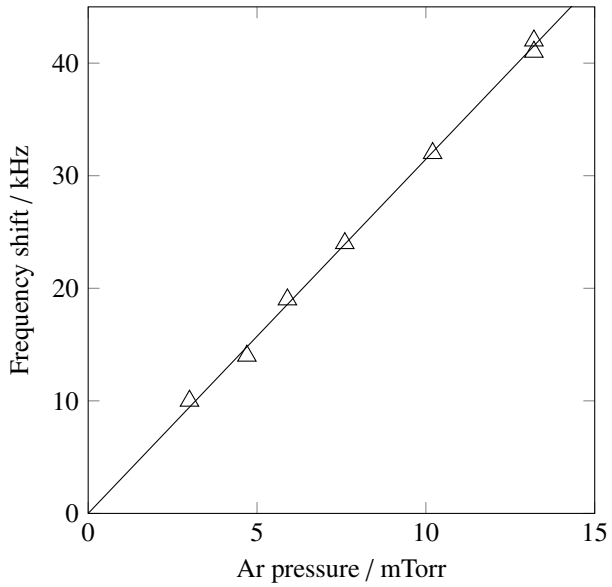

Fig. 2. Frequency shift of the $J = 1 \leftarrow 0$ transition of $^{15}N_2H^+$.

For higher J values, the transition frequencies were obtained by repeated measurements at standard conditions, and their uncertainty resulted to be of a few kHz.

Nine transitions were recorded for $^{15}N_2H^+$, with J from 0 to 12 in the range 88 GHz–1.147 THz, while for the deuterated species the nine transitions detected span the J-value range 3–15 and the frequency range 295 GHz–1.177 THz. The determined experimental transition frequencies were fitted, in an unweighted-least-squares procedure, to the standard frequency expression $J + 1 \leftarrow J$ for the rotational transition:

$$\nu_0 = 2B_0(J+1) - 4D_J(J+1)^3 + H_J(J+1)^3\left[(J+2)^3 - J^3\right], \quad (1)$$

where B_0, D_J, and H_J are the ground-state rotational, quartic, and sextic centrifugal distortion constants, respectively. The values of the spectroscopic constants of $^{15}N_2H^+$ and $^{15}N_2D^+$ derived from the fits are reported in Table 1. Table 1 reports also,

Table 1. Rotational transition frequencies and spectroscopic constants of $^{15}N_2H^+$ and $^{15}N_2D^+$.

		$^{15}N_2H^+$				$^{15}N_2D^+$			
$J+1$	J	Observed (MHz)	Obs.-calc. (kHz)	Uncert.[a] (kHz)	A[b] (s^{-1})	Observed (MHz)	Obs.-calc. (kHz)	Uncert.[a] (kHz)	A[b] (s^{-1})
1	0	88 264.0580	−1.1	0.3	3.08(−5)	73 635.4710[c]		0.3	1.79(−5)
2	1	176 526.2210[c]		0.6	2.96(−4)	147 269.6072[c]		0.5	1.72(−4)
3	2	264 784.5878	−0.8	0.8	1.07(−3)	220 901.0740[c]		0.7	6.22(−4)
4	3	353 037.2641	−0.6	0.9	2.63(−3)	294 528.5363	−0.3	0.8	1.53(−3)
5	4	441 282.3524[c]		0.9	5.26(−3)	368 150.6609	0.3	0.9	3.05(−3)
6	5	529 517.9570	2.2	0.8	9.22(−3)	441 766.1115[c]		0.9	5.35(−3)
7	6	617 742.1767	1.3	0.8	1.48(−2)	515 373.5533	−1.9	0.8	8.60(−3)
8	7	705 953.1169	−0.7	0.9	2.23(−2)	588 971.6577	0.0	0.8	1.29(−2)
9	8	794 148.8830	−2.4	1.1	3.19(−2)	662 559.0842	−0.9	0.7	1.85(−2)
10	9	882 327.5827[c]		1.3	4.40(−2)	736 134.5064	2.2	0.8	2.56(−2)
11	10	970 487.3141[c]		1.3	5.88(−2)	809 696.5838	2.0	1.0	3.42(−2)
12	11	1 058 626.1863	2.0	1.1	7.66(−2)	883 243.9851[c]		1.2	4.45(−2)
13	12	1 146 742.2976	−1.0	1.5	9.77(−2)	956 775.3817[c]		1.3	5.67(−2)
14	13	1 234 833.7625[c]		1.5	1.22(−1)	1 030 289.4371	−2.8	1.2	7.10(−2)
15	14					1 103 784.8281[c]		1.2	8.76(−2)
16	15					1 177 260.2165	1.0	1.7	1.06(−1)
17	16					1 250 714.2716[c]		3.2	1.28(−1)
			rms[d] = 1.5 kHz				rms[d] = 1.6 kHz		

Constant	Value[e]	Correlation matrix			Value[e]	Correlation matrix		
B_0 / MHz	44 132.18765(17)	1.000			36 817.84672(13)	1.000		
D_J / kHz	79.0502(20)	0.934	1.000		55.6152(10)	0.931	1.000	
H_J / mHz	50.4(63)	0.871	0.986	1.000	50.7(22)	0.860	0.982	1.000

Notes. [a] Uncertainties derived from the errors on the fitted spectroscopic parameters. [b] The order of magnitude is reported in parentheses. [c] Predicted value. [d] Root-mean-square error of the residuals: $\sqrt{\frac{\sum \text{residual}^2}{N \text{ observations}}}$. [e] Standard errors are reported in parentheses in units of the last quoted digit.

for the two isotopologues, the lists of observed and predicted rotational transition frequencies up to 1.25 THz.

3. Discussion

3.1. Experimental results

The rotational spectra of the fully ^{15}N-substituted isotopologues of the diazenylium ion have been recorded at millimeter and sub-millimeter wavelengths (88 GHz–1.2 THz). Nine rotational transitions were accurately determined for each isotopologue of the H- and D-containing pair. The determined line positions are accurate, because of the effort made to minimize the significance of the most common sources of systematic error. This reflects on the values of the rms error of fit residuals, 1.5 kHz for $^{15}N_2H^+$ and 1.6 kHz for $^{15}N_2D^+$, which are remarkably low values for Doppler limited measurements.

Thanks to the measurements above 1 THz, the centrifugal analysis has been carried out up to the sextic term: a comparison between the sextic centrifugal distortion constants determined for different isotopologues of N_2H^+ supports its accuracy (see Table 2). Theoretical estimates of the equilibrium value of the sextic centrifugal distortion constant (H_e) have been computed using the CFOUR program package[1], with the adoption of the coupled-cluster singles and doubles approximation augmented by a perturbative treatment of triple excitations (CCSD(T), Raghavachari et al. 1989). The calculation was performed employing augmented quadruple-ζ quality basis sets (i.e., aug-cc-pCVQZ, Woon & Dunning 1994) and correlating all electrons. After geometry optimizations and harmonic force constants evaluation, the cubic force field for all the diazenylium isotopologues was evaluated in the normal-coordinate representation by means of numerical differentiation (Stanton et al. 1998; Stanton & Gauß 2000). Then, 2nd-order perturbation formulas, simplified for linear molecules, were used to compute H_e (Aliev & Watson 1985).

Table 2. Values (mHz) of the sextic centrifugal distortion constant of isotopologues of N_2H^+.

Isotopologue	Experimental	Computed[a]
N_2H^+	73.5(17)[b]	48.8
N_2D^+	71.6(35)[b]	34.2
$^{15}N_2H^+$	50.4(63)[c]	40.1
$^{15}N_2D^+$	50.7(22)[c]	29.8

Notes. [a] "All electron" theoretical calculation done at CCSD(T) level of theory using aug-cc-pCVQ basis set (see text). [b] Yu et al. (2009). [c] This work.

[1] See www.cfour.de

Table 3. Reactions fractionating $^{15}N_2$ species.

No.	Reaction	k_f ($cm^3\ s^{-1}$)	$\Delta E/k$ (K)	$K(T)$ (10 K)
R1	$^{14}N^{15}N + {}^{15}N^+ \leftrightharpoons {}^{15}N_2 + {}^{14}N^+$	2.0×10^{-10}	28.8	8.7
R2a	$^{14}N^{15}NH^+ + {}^{15}N \rightleftharpoons {}^{15}N_2H^+ + {}^{14}N$	2.0×10^{-10}	30.9	21.5
R2b	$^{15}N^{14}NH^+ + {}^{15}N \rightleftharpoons {}^{15}N_2H^+ + {}^{14}N$	2.0×10^{-10}	39.2	48.7
R3a	$^{14}N^{15}NH^+ + {}^{14}N^{15}N \rightleftharpoons {}^{15}N_2H^+ + {}^{14}N_2$	2.0×10^{-10}	2.5	0.64
R3b	$^{15}N^{14}NH^+ + {}^{14}N^{15}N \rightleftharpoons {}^{15}N_2H^+ + {}^{14}N_2$	2.0×10^{-10}	10.8	1.46

Actually, the experimental values of the ^{15}N-containing pair are properly smaller than those of the parent pair; moreover, for both pairs, the values of the hydrogenated and deuterated species are not significantly different. This latter finding is in apparent contrast with the trend exhibited by the computed equilibrium values, for which variations of ∼30% are observed upon H⟷D isotopic substitution. This discrepancy is, however, smaller than the typical magnitude of the zero-point contribution to the sextic centrifugal term of light linear molecules, and thus can be explained by invoking different ro-vibrational effects.

For both $^{15}N_2H^+$ and $^{15}N_2D^+$, the result of our accurate analysis is a very reliable set of rest frequencies, with 1σ uncertainties above 1 THz less than 0.001 km s^{-1}.

The Einstein A-coefficient for spontaneous emission from state $J+1$ to J of a linear molecule can be calculated from the line strengths by use of

$$A_{J+1\to J} = \frac{16\pi^3\nu^3}{3\epsilon_0 hc^3}\frac{S}{2(J+1)+1}\mu^2 = 1.163965422\times10^{-20}\frac{\nu^3 S}{2(J+1)+1}\mu^2\,, \quad (2)$$

where $A_{J+1\to J}$ is in s^{-1}, the transition frequency ν is in MHz, and μ is the dipole moment in Debye units. The line strength S is defined such that $\mu^2 S = |\mu_{ul}|^2$, where μ_{ul} is the matrix element of the dipole-moment operator in the rotational wavefunctions basis. For a linear rotor with no hyperfine structure, the line strength of a transition connecting the $J+1$ and J states is

$$S = \frac{(J+1)^2 - \ell^2}{J+1}\,, \quad (3)$$

which reduces to $S = J+1$ for ground-state lines with no vibrational angular momentum ($\ell = 0$). Assuming that the dipole moment is the same as that of the main isotopologue, $\mu = 3.4\pm0.2$ D (Havenith et al. 1990), the A-coefficient can be computed for each transition. Therefore, along with the lists of rest frequencies, the values of the Einstein A-coefficients are reported in the sixth and last columns of Table 1.

3.2. Potential constraints on fractionation models

What abundance ratios of fully ^{15}N-substituted isotopologues of diazenylium ($^{15}N_2H^+/^{15}NNH^+$ or $^{15}N_2H^+/N^{15}NH^+$) can then be expected to be observed in the ISM? For an upper limit estimate, the chemical reaction network of Wirström et al. (2012) has been updated to include fractionation into the doubly ^{15}N-substituted species through the reactions listed in Table 3.

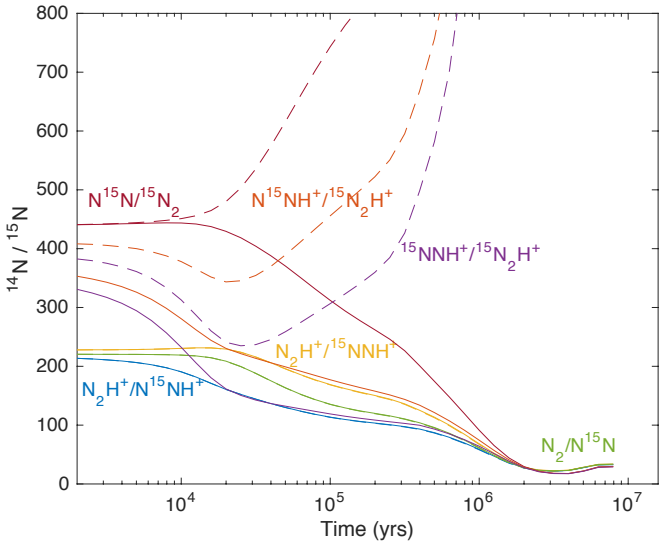

Fig. 3. Nitrogen isotopologue ratios (as labeled) in the doubly substituted species, as well as the singly substituted diazenylium and molecular nitrogen, as predicted when including the fractionating reactions of Table 3 (solid) and not including them (dashed). The red graphs represent $^{15}NN/^{15}N_2$, the orange $N^{15}NH^+/^{15}N_2H^+$, the purple $^{15}NNH^+/^{15}N_2H^+$, the yellow $N_2H^+/^{15}NNH^+$, the blue $N_2H^+/N^{15}NH^+$, and the green $N_2/N^{15}N$.

These reactions have not been studied, so reaction rates, zero-point energy differences ($\Delta E/k$), and equilibrium coefficients ($K(T)$) are unknown and have been ad hoc estimated as given in Table 3 for the purpose of this investigation. The values of ΔE are estimated from the zero-point vibrational energies reported in Table 3 of Mladenović & Roueff (2014) and $K(T)$ is computed using Eq. (5) of Terzieva & Herbst (2000). In the case of reactions R1 and R2, rate constants are assumed based on the corresponding reactions fractionating the singly substituted $^{14}N^{15}N$ and diazenylium in the Wirström et al. (2012) chemical network. Reactions R3 are included as analogs to the reaction $H_2D^+ + HD \leftrightharpoons D_2H^+ + H_2$, which is important in deuteration chemistry, and we simply assumed forward rate coefficients (k_f) similar to the reactions R1 and R2. As in Wirström et al. (2012), the elemental $^{14}N/\,^{15}N$ ratio is assumed to be 440, with 50% of ^{15}N initially in molecular form, but also 1/440 of this (0.23%) is taken to form an initial $^{15}N_2$ pool.

We investigate the effect of including the fractionation reactions R1–R3 under the same physical conditions as in Wirström et al. (2012). Figure 3 compares the temporal evolution of the $^{14}N/^{15}N$ ratio in doubly substituted molecular nitrogen and diazenylium for these two models. It demonstrates that

if there is some direct fractionation, the doubly ^{15}N-substituted species will become enhanced in ^{15}N instead of depleted.

In particular, reactions R2 and R3 both have the effect of producing more $^{15}N_2H^+$ already from early on, thereby lowering the $N^{15}NH^+/^{15}N_2H^+$ and $^{15}NNH^+/^{15}N_2H^+$ ratios. The main production of $^{15}N_2$ is from dissociative electron recombination of $^{15}N_2H^+$, so the $N^{15}N/^{15}N_2$ ratio is only significantly affected when the absolute abundance of diazenylium increases, after about 10^4 yr. Reaction R1, on the other hand, only becomes important as the *ortho*-H_2 abundance drops after about 2×10^5 yr and more $^{15}N^+$ thus becomes available (see Wirström et al. 2012, for a more detailed discussion on the effects of a varying H_2 *ortho*-to-*para* ratio). For the effective fractionation tested here, the abundance ratios $N^{15}NH^+/^{15}N_2H^+$ and $^{15}NNH^+/^{15}N_2H^+$ are predicted to be similar to the $N_2H^+/N^{15}NH^+$ and $N_2H^+/^{15}NNH^+$ at times when their absolute abundances should be largest (10^5–10^6 yr).

As mentioned above, Fontani et al. (2015) reported observations of a few targets (i.e., 05358-mm1, 05358-mm3) where the $N_2H^+/N^{15}NH^+$ ratios are as high as 150–180. These significant ^{15}N-enhancements cannot be accounted for by the latest nitrogen chemistry network (e.g., Roueff et al. 2015), hence, these "anomalous" sources can provide an effective test for updated models. Indeed, considerations based on the trends shown in Fig. 3 suggest that $^{15}N_2H^+$ might be detectable towards 05358-mm1/05358-mm3. The model predicts $N^{15}NH^+/^{15}N_2H^+$ ratios in the range 20–100 at times $>6\times10^5$ yr, therefore, from the column density values of singly ^{15}N-substituted diazenylium determined by Fontani et al. (2015) and taking into account the absence of hyperfine splitting, peak intensities as high as 6 mK can be estimated for $^{15}N_2H^+$. This prediction is well above the sensitivity limit achievable by state-of-the-art millimeter telescopes in a few hours of observation at 0.1–0.3 km s^{-1} spectral resolution.

We note that, from Fig. 3, it can also be deduced that while the abundance of $^{15}N_2H^+$ can be expected to be significantly elevated above elemental at all times if reactions R1–R3 are viable, this only has a minor effect on the $N_2H^+/N^{15}NH^+$ and $N_2H^+/^{15}NNH^+$ ratios. These are at most elevated by 2% at times later than 8×10^5 yr, so inclusion of fractionation to doubly ^{15}N-substituted species cannot reproduce the whole range of ^{15}N enhancements in singly-substituted diazenylium observed by Fontani et al. (2015).

4. Conclusions

We have used high-resolution laboratory spectroscopy techniques to accurately study the rotational spectra of the multiply isotopically substituted versions of the diazenylium ions, $^{15}N_2H^+$ and $^{15}N_2D^+$. This latter has been spectroscopically characterized for the first time. Very accurate rest frequencies are provided in the frequency region 88 GHz–1.2 THz to support astronomical searches for this doubly ^{15}N-containing species. Our understanding of interstellar ^{15}N fractionation is clearly incomplete (Roueff et al. 2015; Wirström et al. 2016) but, as we have shown here, a simplistic scenario for ion-molecule fractionation does predict a significant enrichment of ^{15}N in $^{15}N_2H^+$. Observational constraints on $^{15}N_2H^+$ abundances based on these spectroscopic data will be crucial for ameliorating theoretical problems with interstellar ^{15}N fractionation chemistry.

Acknowledgements. This work has been supported by MIUR (PRIN12 "STAR: Spectroscopic and computational Techniques for Astrophysical and Atmospheric Research" (grant number 20129ZFHFE) and by the University of Bologna (RFO funds).

References

Adande, G. R., & Ziurys, L. M. 2012, ApJ, 744, 194
Aliev, M. R., & Watson, J. K. G. 1985, in Molecular Spectroscopy: Modern Research, Vol. III, ed. K. N. Rao (New York: Academic Press), 1
Bizzocchi, L., Caselli, P., Leonardo, E., & Dore, L. 2013, A&A, 555, A109
Bockelée-Morvan, D., Calmonte, U., Charnley, S., et al. 2015, Space Sci. Rev., 197, 47
Briani, G., Gounelle, M., Marrocchi, Y., et al. 2009, Proc. Nat. Acad. Sci., 106, 10522
Cazzoli, G., Cludi, L., Buffa, G., & Puzzarini, C. 2012, ApJS, 203, 11
Dore, L., Bizzocchi, L., Degli Esposti, C., & Tinti, F. 2009, A&A, 496, 275
Fontani, F., Caselli, P., Palau, A., Bizzocchi, L., & Ceccarelli, C. 2015, ApJ, 808, L46
Füri, E., & Marty, B. 2015, Nature Geoscience, 8, 515
Gudeman, C. S. 1982, Ph.D. Thesis, University of Wisconsin-Madison, USA
Havenith, M., Zwart, E., Leo Meerts, W., & Ter Meulen, J. J. 1990, J. Chem. Phys., 93, 8446
Hily-Blant, P., Bonal, L., Faure, A., & Quirico, E. 2013, Icarus, 223, 582
Marty, B., Chaussidon, M., Wiens, R. C., Jurewicz, A. J. G., & Burnett, D. S. 2011, Science, 332, 1533
Mladenović, M., & Roueff, E. 2014, A&A, 566, A144
Mumma, M. J., & Charnley, S. B. 2011, ARA&A, 49, 471
Nier, A. O. 1950, Phys. Rev., 77, 789
Raghavachari, K., Trucks, G. W., Pople, J. A., & Head-Gordon, M. 1989, Chem. Phys. Lett., 157, 479
Ritchey, A. M., Federman, S. R., & Lambert, D. L. 2015, ApJ, 804, L3
Rodgers, S. D., & Charnley, S. B. 2008, MNRAS, 385, L48
Roueff, E., Loison, J. C., & Hickson, K. M. 2015, A&A, 576, A99
Stanton, J. F., & Gauß, J. 2000, Int. Rev. Phys. Chem., 19, 61
Stanton, J. F., Lopreore, L., & Gauß, J. 1998, J. Chem. Phys., 108, 7190
Terzieva, R., & Herbst, E. 2000, MNRAS, 317, 563
Wirström, E. S., Charnley, S. B., Cordiner, M. A., & Milam, S. N. 2012, ApJ, 757, L11
Wirström, E., Milam, S., Adande, G., Charnley, S. B., & Cordiner, M. A. 2015, IAU General Assembly, 22, 2254599
Wirström, E. S., Adande, G., Milam, S. N., Charnley, S. B., & Cordiner, M. A. 2016, IAU Focus Meeting, 29, 271
Woon, D. E., & Dunning, T. H. 1994, J. Chem. Phys., 100, 2975
Yu, S., Pearson, J. C., Drouin, B. J., et al. 2009, J. Mol. Spectrosc., 314, 19